Vibrational Spectra and Structure of CH_3Cl:NO Complex: IR Matrix Isolation and DFT Study

Nadia Dozova, Lahouari Krim,* M. Esmaïl Alikhani, and Nelly Lacome

Université Pierre et Marie Curie, CNRS UMR 7075/Ladir, Bâtiment F74, case 49, 4 place Jussieu, 75252 Paris, Cedex 05, France

Received: July 15, 2005; In Final Form: October 4, 2005

Infrared spectra of the CH_3Cl:NO complex isolated in solid neon have been investigated. Most of the vibrational modes of the complex have been detected. The weak interaction between NO and CH_3Cl in CH_3Cl:NO is responsible for small shifts of the vibrational mode frequencies of both CH_3Cl and NO molecules. The measured shifts range between -3.2 and $+3.8$ cm^{-1}. On the basis of DFT calculations, different geometries have been explored for the complex, and it has been shown that the most stable structure is of C_1 symmetry. The calculated frequency shifts match well the experimental data.

Introduction

A fraction of methyl chloride (CH_3Cl) molecules (atmospheric lifetime 2−3 years)[1] produced by photosynthetic algae reaches the stratosphere and is then oxidized by various molecules or radicals. CH_3Cl oxidation mechanisms have been the subject of different studies.[2−7] Schriver et al.[3] studied the reaction between atomic oxygen in its ground and excited states with CH_3Cl. Reactions of the molecular ion OH^- with CH_3X (X = halogen atoms) have been investigated by several groups.[4−6] Recent studies[2,7] showed that the oxidation of CH_3Cl yields different products depending on whether the reaction is done in the presence or absence of molecules of NO.

The goal of this work is to try to understand if there is any interaction between NO and CH_3Cl. Rare gas matrix isolation technique coupled with infrared spectroscopy (IR) is well adapted for the observation of a system like this one because it makes possible the detection of both intermediates and products of reaction, in particular if the lifetimes of these species are short.

Infrared spectra of NO + CH_3Cl isolated in solid neon at low temperature have been recorded. The NO + CH_3Cl system has a remarkable propensity to form $(NO)_2$,[8] CH_3Cl:NO, CH_3Cl:$(NO)_2$, and $(CH_3Cl)_2$,[9] and IR spectroscopy reveals a variety of phenomena far from being fully understood.

We will focus here only on the CH_3Cl:NO species. Low concentration studies and subsequent annealing lead to the formation of 1:1 CH_3Cl:NO van der Waals complex. The vibrational modes of this complex have been detected. Density functional calculations of the geometric and vibrational properties of the complex will be also presented and compared to experimental values.

Experimental Technique

The CH_3Cl + NO samples were prepared by co-condensing CH_3Cl/NO/Ne mixtures onto a cryogenic metal mirror maintained at 5 K. Molar ratios (X/Ne: X = CH_3Cl or NO) ranged from 0.001% to 1%. The experimental methods and setup have been previously described in detail.[10] Deposition times were around 60 mn. Neon, CH_3Cl, and ^{14}NO gases were obtained from L'Air liquide with purities of 99.9995%, 99.8%, and 99.9%, respectively. ^{15}NO gas was provided by Isotec with an isotopic purity of 97.8%. $^{14}N^{18}O$ was prepared in the laboratory by addition of $^{18}O_2$ to $^{14}N^{16}O$ gas to form $^{14}N^{(16+18)}O_2$ which was subsequently reduced to $^{14}N^{18}O$ and $^{14}N^{16}O$ by reaction with mercury. In all samples, NO gas, its isotopomers, and CH_3Cl were purified by using trap-to-trap vacuum distillations. The purity of samples was confirmed spectroscopically.

Infrared spectra of the resulting samples were recorded in the transmission-reflection mode between 4500 and 500 cm^{-1} using a Bruker 120 FTIR spectrometer equipped with a KBr/Ge beam splitter and a liquid N_2 cooled narrow band HgCdTe photoconductor. A resolution of 0.1 cm^{-1} was used. Bare mirror backgrounds, recorded from 4500 to 500 cm^{-1} prior to sample deposition, were used as references in processing the sample spectra. Absorption spectra in the midinfrared were collected on samples through a KBr window mounted on a rotatable flange separating the interferometer vacuum (10^{-3} mbar) from that of the cryostatic cell (10^{-7} mbar). The spectra were subsequently subjected to baseline correction to compensate for infrared light scattering and interference patterns.

For each sample, corresponding to different concentrations of CH_3Cl and NO, or different isotopic precursors, three kinds of spectra were recorded at 5 K after each of the following procedures: (1) after sample deposition; (2) after warming the matrix at several steps to 12 K to vary and monitor the formation of higher stoechiometry complexes; (3) after irradiating the sample using a 200 W mercury−xenon high-pressure arc lamp and either interference narrow (5 nm full width at half-maximum) or broad-band filters to find if some photoprocesses could be initiated by UV−visible or near-infrared light.

Experimental Results

NO in Ne Matrix. The spectrum of NO in neon matrix has been extensively studied by Kometer et al.[11] In our experiments NO/Ne was deposited at 5 K. The stretching of the NO monomer consists of two bands: peak I (intense) at 1874.6 cm^{-1} and peak II (weaker) at 1877.5 cm^{-1} (Figure 1a). These peaks correspond to NO in single and NO in double or triple substitutional sites of the neon matrix, respectively.[11] Upon annealing other bands

* To whom correspondence should be addressed. E-mail: krim@ccr.jussieu.fr.

10.1021/jp053894o CCC: $30.25
Published on Web 11/11/2005

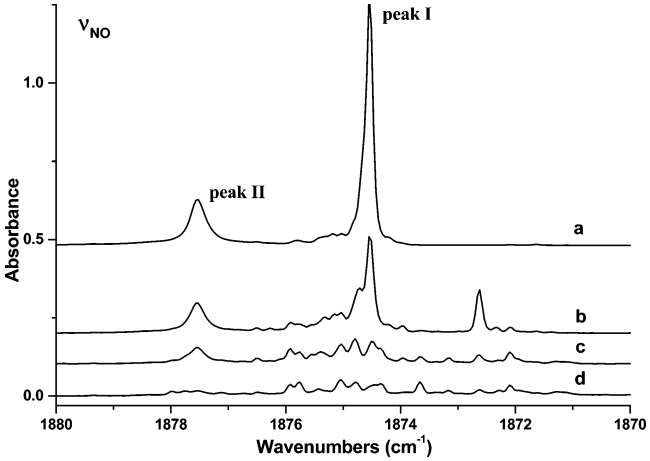

Figure 1. Annealing effects on the spectrum of NO monomer (υ_{NO}) for a sample with NO/Ne = 5/10000: (a) after deposition at 5 K; (b) after annealing to 9 K; (c) after annealing to 10 K; (d) after annealing to 11 K. All spectra were recorded at 5 K.

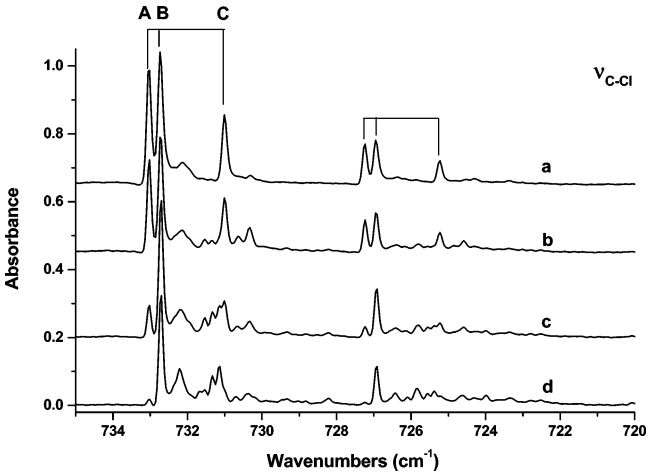

Figure 2. Annealing effects on the spectrum of CH_3Cl in the C−Cl stretching (υ_3) region for a sample with CH_3Cl/Ne = 5/10000: (a) after deposition at 5 K; (b) after annealing to 10 K; (c) after annealing to 11 K; (d) after annealing to 12 K. All spectra were recorded at 5 K.

corresponding to the NO monomer appear in this region (Figure 1b−d). They have been assigned to monomers that are close together, but hindered by the matrix cage from forming the NO dimer.[11] Other broad absorptions belonging to cis-$(NO)_2$ are present in our spectra at 1865 cm^{-1} (symmetric NO stretching) and 1779.6 cm^{-1} (antisymmetric NO stretching).[11]

CH_3Cl in Ne Matrix. Spectra of CH_3Cl isolated in neon matrix have been recorded at 5 K at different concentrations of CH_3Cl. Figure 2 shows the C−Cl stretching region after sample annealing up to 12 K in several steps. The C−Cl stretching region has two sets of bands belonging to the two isotopomers $CH_3{}^{35}Cl$ and $CH_3{}^{37}Cl$. Each band consists of three sharp peaks probably due to splitting by the matrix cage. For the $CH_3{}^{35}Cl$ isotopomer they are situated at 733.0 cm^{-1} (peak A), at 732.7 cm^{-1} (peak B with shoulder), and at 731.0 cm^{-1} (peak C with shoulder), while for the other isotopomer they are situated at 727.2, 726.9, and 725.2 cm^{-1}, respectively (Figure 2a). The shift between the corresponding peaks in the two isotopomers is 5.8 cm^{-1}. At the temperature of deposition (T = 5 K), peaks A and B are equally intense, and peak C is weaker (Figure 2a). Annealing changes the relative intensities of peaks A, B, and C. New peaks grow in the region of peak C (Figure 2b,c). They are probably due to CH_3Cl molecules interacting with each other, but sufficiently far away to not form the CH_3Cl dimer (similar to what is observed in the case of NO in Ne matrix[11]). At 11−12 K (Figure 2d), peak A disappears and peak B is the most intense, thus showing that it is the most stable site of CH_3Cl trapped in the matrix. At higher concentration other peaks appear between 726 and 722 cm^{-1}. The behavior of their intensities suggests that they belong to $(CH_3Cl)_2$.

In the region of C−H symmetric stretching (and also for other vibrational modes of CH_3Cl), three peaks are observed; each of them is correlated with one of the peaks A, B, and C in the C−Cl stretching mode region. The frequencies of the modes of CH_3Cl trapped in the most stable site in neon matrix (site B) are given in Table 1.

CH_3Cl:NO Complex in Ne Matrix. *C−Cl Stretching Region.* When CH_3Cl and NO are co-deposited in neon matrix, two new bands appear in the C−Cl stretching region (Figure 3α). The ratio of their relative intensities is equal to 3/1 and corresponds to the isotopic abundance of chlorine ($^{35}Cl/^{37}Cl$). These bands grow linearly with both CH_3Cl and NO concentrations and may be assigned to the complex CH_3Cl:NO. These bands show a strong dependence on the temperature of the matrix. Annealing from 5 to 9 K shows the growth of a three-peak structure in the region of $CH_3{}^{35}Cl$:NO and $CH_3{}^{37}Cl$:NO (Figure 3β). They are located at 729.9, 729.5, and 727.6 cm^{-1} for $CH_3{}^{35}Cl$:NO and at 724.1, 723.7, and 721.9 cm^{-1} for $CH_3{}^{37}$-Cl:NO. The distribution of these peaks is similar to the structure of the absorption bands of CH_3Cl in neon matrix where the three peaks A, B, and C belong to different sites in the matrix occupied by CH_3Cl. To the absorption peaks A (733.0 cm^{-1}), B (732.7 cm^{-1}), and C (731.0 cm^{-1}) of $CH_3{}^{35}Cl$ correspond the three peaks A (729.9 cm^{-1}), B (729.5 cm^{-1}), and C (727.6 cm^{-1}) of $CH_3{}^{35}Cl$:NO. In the same way, the peaks A (727.2 cm^{-1}), B (726.9 cm^{-1}), and C (725.2 cm^{-1}) of $CH_3{}^{37}Cl$ correspond to the peaks A (724.1 cm^{-1}), B (723.7 cm^{-1}), and C (721.9 cm^{-1}) of $CH_3{}^{37}Cl$:NO. Beyond 11 K the absorption peak B is the most intense in CH_3Cl and in the complex CH_3-Cl:NO (Figure 3γ). Peak B in CH_3Cl represents the most stable site of CH_3Cl at 11 K, and peak B of the complex represents the most stable site of CH_3Cl:NO. In the regions of the other modes of CH_3Cl, the bands of CH_3Cl:NO have been found to correlate with peaks A, B, and C in the C−Cl stretching region. Table 1 gathers the vibrational mode frequencies of CH_3Cl and CH_3Cl:NO in the most stable site at high temperature: site B.

N−O Stretching Region. In the NO stretching region (Figure 4α and Figure 5) a series of new peaks appears on both sides of peak II of NO: at 1878.5, 1878.4, 1877.9 (shoulder to peak II), 1877.4 (very weak), 1876.7, 1876.5, and 1876.2 cm^{-1}. They all increase linearly with CH_3Cl and NO concentrations (Figure 4α and Figure 5). Figure 4 shows the evolution of these peaks as a function of CH_3Cl concentration and of the temperature of the matrix. All these peaks grow when the matrix is annealed from 5 to 9 K except for the peak at 1876.2 cm^{-1}, which decreases (Figure 4β). In this temperature range, peak I of NO strongly decreases, while peak II remains almost constant. Beyond 11 K only the peak at 1878.4 cm^{-1} remains intense (Figure 4γ). Among the peaks that depend on CH_3Cl and NO in the NO stretching region, three peaks have been found to correlate with the three peaks A, B, and C attributed to CH_3-Cl:NO in the C−Cl stretching region. These peaks are located at 1878.5 (A), 1878.4 (B), and 1877.4 cm^{-1} (C) and are due to the NO stretching of the complex CH_3Cl:NO trapped in the neon matrix. As in the C−Cl stretching region only peak B, corresponding to the most stable site of CH_3Cl:NO, remains intense beyond 11 K. Table 1 shows the frequencies of the

TABLE 1: Vibrational Mode Frequencies (in cm^{-1}) of CH_3Cl (site B), NO and CH_3Cl:NO (site B) Complex in Neon Matrix

mode		CH_3Cl/Ne	NO/Ne	CH_3Cl:NO/Ne	shift[a]
C−Cl stretching	$\upsilon_3(A_1)$	732.7 ^{35}Cl, 726.9 ^{37}Cl		729.5 ^{35}Cl, 723.7 ^{37}Cl	−3.2
C−Cl rocking	$\upsilon_6(E)$	1019.4		1022.2	+2.8
C−H symmetric bending	$\upsilon_2(A_1)$	1354.8		1354.3	−0.5
C−H antisymmetric bending	$\upsilon_5(E)$	1450.1		1448.4	−1.7
C−H symmetric stretching	$\upsilon_1(A_1)$	2967.4		2969.8	+2.4
C−H antisymmetric stretching	$\upsilon_4(E)$	3036.8		*b*	
N−O stretching	υ_{NO}		1874.6 (peak I), 1877.5 (peak II)	1878.4	+3.8

[a] Shift = $\upsilon_{complex} - \upsilon_{free\ molecule}$. [b] Only a broadening of the bands of CH_3Cl was observed.

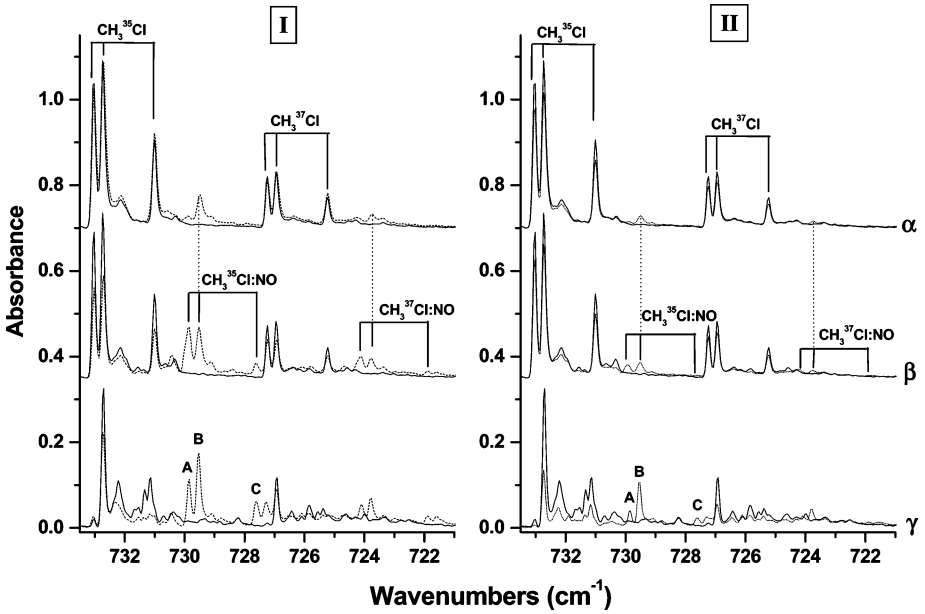

Figure 3. Annealing effects on CH_3Cl:NO bands in the C−Cl stretching mode (υ_3) region: (α) after deposition at 5 K; (β) after annealing to 9−10 K; (γ) after annealing to 11−12 K. All spectra were recorded at 5 K. I panel: ---, CH_3Cl/NO/Ne = 5/10/10000; —, CH_3Cl/Ne = 5/10000. II panel: ···, CH_3Cl/NO/Ne = 5/5/10000; —, CH_3Cl/Ne = 5/10000.

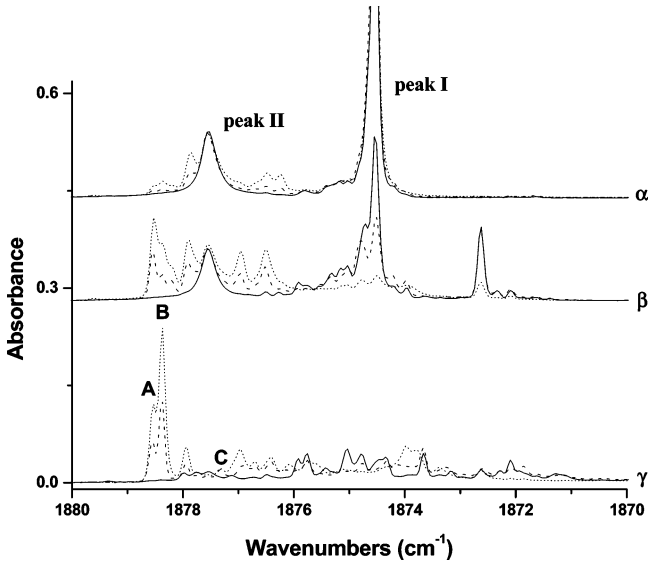

Figure 4. Annealing effects on CH_3Cl:NO bands in the NO stretching mode (υ_{NO}) region: (α) after deposition at 5 K; (β) after annealing to 9 K; (γ) after annealing to 11 K. All spectra were recorded at 5 K. —, NO/Ne = 5/10000; ---, CH_3Cl/NO/Ne = 5/5/10000; ···, CH_3Cl/NO/Ne = 20/5/10000.complex.

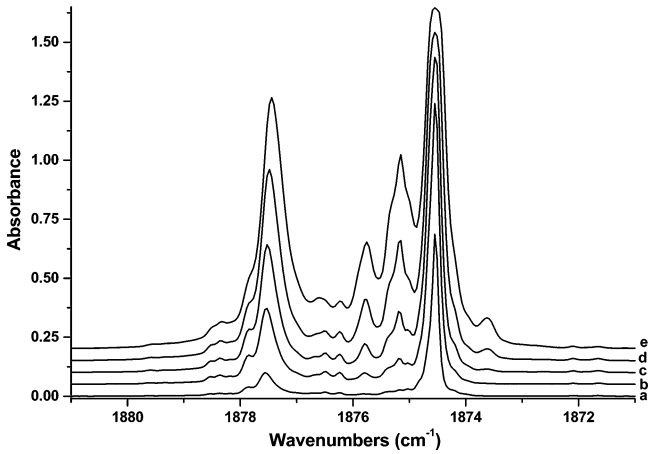

Figure 5. Effects of NO concentration on CH_3Cl:NO bands in the NO stretching mode (υ_{NO}) region: (a) NO/CH_3Cl/Ne = 5/5/10000; (b) NO/CH_3Cl/Ne = 10/5/10000; (c) NO/CH_3Cl/Ne = 20/5/10000; (d) NO/CH_3Cl/Ne = 40/5/10000; (e) NO/CH_3Cl/Ne = 100/5/10000.

vibrations of NO, CH_3Cl, and CH_3Cl:NO in neon matrix in the most stable site (site B).

Upon co-deposition of CH_3Cl with ^{15}NO, with a mixture of ^{14}NO and ^{15}NO or with a mixture of $N^{16}O$ and $N^{18}O$, no change of the frequencies of the bands in the regions of the CH_3Cl modes was observed. The structure of the bands of CH_3Cl:^{15}NO and CH_3Cl:$N^{18}O$ in the ^{15}NO and $N^{18}O$ stretching regions, respectively, is the same as the one of CH_3Cl:$^{14}N^{16}O$ in the $^{14}N^{16}O$ stretching region. The same shifts between the bands of the complexes and free NO molecules are observed for each isotopomer. Figure 6 shows a comparison of the complex bands in the ^{14}NO and ^{15}NO stretching modes regions for a ^{14}NO/^{15}NO/CH_3Cl/Ne mixture after annealing to 9 K.

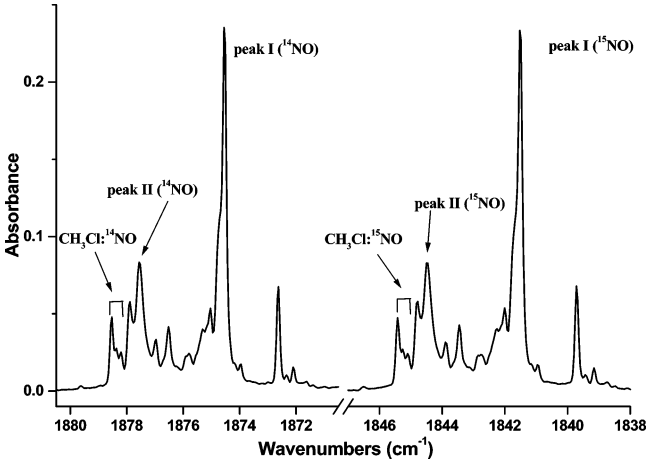

Figure 6. Spectra of ^{14}NO and ^{15}NO stretching mode (υ_{NO}) regions for a sample: ^{14}NO/^{15}NO/CH_3Cl/Ne = 5/5/5/10000 after annealing to 9 K.

Finally, CH_3Cl:NO complex was irradiated by UV−visible or near-infrared light to initiate some photoprocesses, but no photochemical reactions were observed.

Discussion

CH_3Cl occupies three different sites labeled A, B, and C in the neon matrix. When CH_3Cl and NO are co-deposited in neon matrix, the complex CH_3Cl:NO also occupies three sites A, B, and C. The bands of the complex in the CH_3Cl and NO vibrational mode regions are observed for each site (A, B, and C). At the temperature of deposition the complex occupies mainly site B. After annealing (6−10 K) the NO molecules diffuse through the matrix to CH_3Cl trapped in different sites: the complex CH_3Cl:NO is formed in sites A, B, and C and the bands corresponding to these sites grow. Beyond 10 K the intensity of the peak corresponding to site B increases considerably. By considering site B to be the most stable site in the neon matrix, the shifts of the vibrational mode frequencies of the CH_3Cl:NO and CH_3Cl trapped in site B are given in Table 1. In the CH_3Cl absorption region, the C−Cl (υ_3 at 732.7 cm^{-1}) and C−H (υ_1 at 2967.4 cm^{-1}) symmetric modes are shifted by −3.2 and +2.4 cm^{-1}, respectively, and the CH symmetric bending mode (υ_2 at 1354.8 cm^{-1}) is shifted by −0.5 cm^{-1}. The bands of the modes of symmetry E are shifted by +2.8 cm^{-1} for the C−Cl rocking mode (υ_6 at 1019.4 cm^{-1}) and by −1.7 cm^{-1} for the C−H antisymmetric bending mode (υ_5 at 1450.1 cm^{-1}). For the C−H antisymmetric stretching mode (υ_4 at 3036.8 cm^{-1}), no shift could be measured but only a broadening of the band of CH_3Cl was observed.

The annealing of the matrix promotes the phenomenon of diffusion to form the CH_3Cl:NO complex starting from free molecules CH_3Cl and NO. Between 5 and 10 K the intensity of peak I of the NO monomer decreases considerably, whereas that of peak II remains constant (as shown in Figure 4β). This shows that, in this temperature range, the complex is formed mainly from the NO molecules trapped in site I, corresponding to the principal absorption band of NO. The frequency of the NO stretching mode in the complex trapped in site B is shifted by +3.8 cm^{-1} compared to that of NO:Ne (υ_{NO} at 1874.6 cm^{-1}).

Three very weak peaks appear at deposition of the mixture of CH_3Cl and NO in neon matrix: in the C−Cl stretching region at 727.9 cm^{-1}, in the symmetric C−H stretching region at 2976.2 cm^{-1}, and in the NO stretching region at 1876.2 cm^{-1}. When the matrix is annealed to 9 K, these peaks disappear. They could be attributed to an unstable form of the complex CH_3Cl:NO. Corresponding bands for this species in the other modes of CH_3Cl are not observed. They are probably hidden by the CH_3Cl absorptions.

The three bands in the NO stretching region at 1877.9, 1876.7, and 1876.5 cm^{-1} (Figure 4) do not have corresponding bands in the CH_3Cl vibrational modes regions (probably hidden by the CH_3Cl bands), even though they depend linearly on the concentration of CH_3Cl. These bands are probably due to NO molecules interacting weakly with CH_3Cl.

Theoretical Calculations

All calculations have been performed with the Gaussian 03 quantum chemical package[12] using various levels of theory with the unrestricted wave function: second-order Møller−Plesset perturbation theory (denoted as MP2), and density functional (DFT) approaches. In this paper, two functionals, well adapted to the study of weakly bound systems, have been used: the one-parameter hybrid functional due to Barone's modified functional (labeled as MPW1PW91),[13] and a recent hybrid DFT-type functional, developed in the Truhlar group[14−16] (labeled as MPWB1K, available with Gaussian 03 using the following keywords: "#P mpwb95/basis IOp(3/76=0560004400)"). For all atoms, the 6-311++G(2d,2p) extended basis set of Pople et al.[17−19] was used.

It is interesting to note that the MP2 method is unable to determine the vibrational frequency of free and complexed NO. In the case of free NO, the calculated value with MP2 is around 3550 cm^{-1} instead of 1904 cm^{-1} (the experimental value[20]). It is also well-known that this ill representation does not depend on the basis set.[21] However, to check the reliability of the energetic ordering for the studied complexes obtained with MP2 method, we carried out the single-point calculations at the coupled-cluster level including single and double excitations with the perturbative triple excitation (labeled as CCSD(T)).

As shown in Table 2, the calculated frequencies for the free molecules are in good agreement with the experimental ones, except the MP2 result for free NO. This is why in the following we consider only the energetic properties of the complexes at the MP2 level.

To determine the most stable structure of the CH_3Cl:NO complex, two global geometries have been considered: the first one is of C_1 symmetry in which the NO axis is nearly parallel with the CCl one, and the second one has a C_{3v} symmetry in which the NO and CCl axes are collinear. For each geometry, two structures with respect to NO have been taken into account (see Figure 7). It should be noted that the Cl-ending approach was found to be unbound and thus is not presented here. In the case of the C_1 structure, the optimization has been made without symmetry constraint. This means that the NO and CCl axes were initially chosen to form a small dihedral angle.

The most important geometric parameters of the four studied complexes (see Figure 7) are reported in Table 3. One can easily note that the geometric perturbations induced upon complexation are very small, indicating a very loose bonding between NO and CH_3Cl, for all the studied cases. These changes are in line with the calculated binding energies (corrected for the basis set superposition error (BSSE)), which range from 0.6 to 3.5 kJ mol^{-1}. Accordingly, the most stable geometry formed from the NO + CH_3Cl interaction should be considered as a van der Waals complex. Inspecting the results, reported in Table 3, reveals that the geometric and energetic properties calculated with the new functional of Truhlar are closer to those obtained by MP2 and CCSD(T) than those obtained with the MPW1PW91 functional.

TABLE 2: Calculated and Experimental Frequencies (cm^{-1}) for Free CH_3Cl and NO

	CCSD(T)	MP2	MPW1PW91	MPWB1K	exptl[a]
			Free NO		
ω	2062	3550	2009	2092	1904
			Free CH_3Cl		
$\omega_1(A_1)$	3128	3115	3102	3156	2968
ω_2	1443	1443	1382	1409	1355
ω_3	751	785	747	770	733
$\omega_4(E)$	3236	3223	3203	3260	3044
ω_5	1515	1491	1487	1514	1488
ω_6	1059	1066	1032	1051	1018

[a] The gas-phase experimental frequencies are from refs 20 and 23 for free NO and CH_3Cl, respectively.

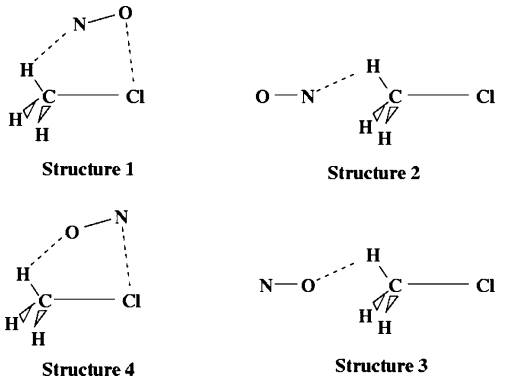

Figure 7. The four different structures studied for the CH_3Cl:NO complex.

TABLE 3: Calculated Geometric Parameters[a] and Stability of the Four Structures of the CH_3Cl:NO Complex

	MP2	MPW1PW91	MPWB1K
		NO	
r_{NO}	1.135	1.141	1.130
		CH_3Cl	
r_{CCl}	1.776	1.784	1.770
		Structure 1	
r_{NO}	1.135	1.141	1.130
r_{CCl}	1.777	1.785	1.771
$r_{H\cdots N}$	2.762	2.996	2.808
D_e^{BSSE}	3.0 (2.8)[b]	1.7	3.5
		Structure 2	
r_{NO}	1.133	1.141	1.130
r_{CCl}	1.778	1.785	1.771
$r_{H\cdots N}$	3.068	3.730	3.712
D_e^{BSSE}	1.6 (−0.5)[b]	0.9	1.2
		Structure 3	
r_{NO}	1.136	1.142	1.131
r_{CCl}	1.776	1.784	1.771
$r_{H\cdots O}$	2.999	3.674	3.510
D_e^{BSSE}	0.8 (−0.5)[b]	0.9	1.0
		Structure 4	
r_{NO}	1.135	1.142	1.131
r_{CCl}	1.776	1.784	1.771
$r_{H\cdots O}$	2.725	3.111	3.133
D_e^{BSSE}	0.6 (1.3)[b]	1.0	1.2

[a] r in Å, D_e^{BSSE} in kJ mol^{-1}. [b] Bonding energy (uncorrected for BSSE) with single-point CCSD(T) at the MP2 optimized geometry.

At all levels of theory, the most stable structure corresponds to the C_1 structure in which NO is nearly parallel to the CCl axis and N is pointing to the carbon atom (structure 1). The dihedral angle between NO and CCl is almost negligible (smaller than 10°). As shown previously,[22] the HNO molecule is more stable than the NOH molecule, and the ClNO molecule is more stable than the NOCl molecule. The geometries of HNO and ClNO units in the most stable complex resemble that of the two most stable forms of HNO and ClNO molecules. For instance, the angles in the complex (−HNO = 149°, −HON = 23°, −ClNO = 112°, and −ClON = 53°) are similar to those of free HNO and ClNO molecules (−HNO = 109°, −HON = 33° and −ClNO = 114°, −ClON = 43°)[22] and not those of the NOCl and NOH molecules (−HNO = 28°, −HON = 112° and −ClNO = 40°, −ClON = 121°).[22]

TABLE 4: Calculated and Experimental Shifts (cm^{-1}) of Vibrational Frequencies of the Most Stable Structure of the Complex (Structure 1)

mode	MPW1PW91		exptl[a]
C−Cl stretching	−2.5	$\upsilon_3(A_1)$	−3.2
C−Cl rocking	1.2, 2.3	$\upsilon_6(E)$	−, 2.8
C−H symmetric bending	−0.1	$\upsilon_2(A_1)$	−0.5
C−H antisymmetric bending	−0.8, 1.0	$\upsilon_5(E)$	−1.7, −
N−O stretching	1.5	υ_{NO}	3.8
C−H symmetric stretching	1.0	$\upsilon_1(A_1)$	2.4
C−H antisymmetric stretching	1.5, 3.1	$\upsilon_4(E)$	−, −

[a] In neon matrix (this work).

The harmonic frequency shifts calculated with the MPW1PW91 method for structure 1 of the complex and the experimental shifts in neon matrix are listed in Table 4.

It has already been shown that experimental shifts of the vibrational mode frequencies of the complex are small. Since the calculations show that the interaction between CH_3Cl and NO is very weak, it is to be expected that the calculated shifts will also be small. Indeed, the largest calculated shift is around 3 cm^{-1}. We will be then mostly interested in the sign of the shifts and not in their absolute value. The frequencies of the C−Cl stretching and the C−H symmetric bending modes are both red shifted upon complexation. The calculated shifts $\Delta\omega_3$ (C−Cl) = −2.5 cm^{-1} and $\Delta\omega_2$ (C−H symmetric bending) = −0.1 cm^{-1} are close to the experimental values $\Delta\upsilon_3 = -3.2$ cm^{-1} and $\Delta\upsilon_2 = -0.5$ cm^{-1}. By contrast, the frequencies of the N−O stretching and the C−H symmetric stretching modes are blue shifted. The calculated values $\Delta\omega_{NO} = +1.5$ cm^{-1} and $\Delta\omega_1$ (C−H symmetric stretching) = +1.0 cm^{-1} are again in good agreement with the values measured in neon matrix, $\Delta\upsilon_{NO} = +3.8$ cm^{-1} and $\Delta\upsilon_1 = +2.4$ cm^{-1}.

Since the complex belongs to the C_1 symmetry group, the modes of symmetry E (in free CH_3Cl) are not degenerate anymore and two different frequencies are calculated for the rocking, C−H antisymmetric bending, and C−H antisymmetric stretching modes. However, only one frequency was experimentally observed for each mode in the complex, except for the C−H antisymmetric stretching where only a broadening of the bands was detected. Furthermore, the absorption bands of CH_3Cl trapped in neon matrix corresponding to these modes are broad and could hide the other absorption bands of the complex. Finally, we note that the experimental frequency shifts for the C−Cl rocking (+2.8 cm^{-1}) and C−H antisymmetric

bending (-1.7 cm^{-1}) modes are well reproduced by DFT calculations (C−Cl rocking $+2.3$ cm^{-1} and C−H bending -0.8 cm^{-1}).

Conclusion

The infrared spectra of NO + CH_3Cl isolated in solid neon at low temperature have been investigated. We focused here on the CH_3Cl:NO species. Low concentration studies and subsequent annealing lead to the formation of 1:1 NO:CH_3Cl van der Waals complex. The vibrational modes of this complex have been detected.

It has been shown that the experimentally observed complex is a van der Waals complex (the binding energy is around 200 cm^{-1}) and that the most stable structure of CH_3Cl:NO (in which NO is nearly parallel to the CCl axis and N is pointing to the carbon atom) belongs to the C_1 group. Observed frequency shifts are well reproduced by use of the hybrid functional (MPW1PW91). According to the experimental and theoretical results, vibrational frequencies are very slightly shifted upon formation of the complex, but with opposite signs: blue and red shifts for the N−O and C−Cl stretching modes, respectively.

References and Notes

(1) Singh, H. B.; Salas, L. J.; Shigeishi, H.; Scribner, E. *Science* **1979**, *203*, 899−903.

(2) Bilde, M.; Orlando, J. J.; Tyndall, G. S.; Wallington, T. J.; Hurley, M. D.; Kaiser, E. W. *J. Phys. Chem A* **1999**, *103*, 3963−3968.

(3) Schriver-Mazzuoli, L.; Schriver, A.; Hannachi, Y. *J. Phys. Chem A* **1998**, *102*, 10221−10229.

(4) Mayhew, C. A.; Peverall, R.; Timperley, C. M.; Watts, P. *Int. J. Mass. Spectrom.* **2004**, *233*, 155−163.

(5) Tachikawa, H.; Igarashi, M.; Ishibashi, T. *J. Phys. Chem A* **2002**, *106*, 10977−10984.

(6) Hierl, P. M.; Henchman, M. J.; Paulson, J. F. *Int. J. Mass Spectrom. Ion Processes* **1992**, *117*, 475−485.

(7) Weller, R.; Lorenzen-Schmidt, H.; Schrems, O. *Ber. Bunsen-Ges. Phys. Chem.* **1992**, *96*, 409−413.

(8) Krim, L.; Lacome, N. *J. Phys. Chem. A* **1998**, *102*, 2289−2296.

(9) Futami, Y.; Kudoh, S.; Ito, F.; Nakanaga, T.; Nakata, M. *J. Mol. Struct.* **2004**, *690*, 9−16.

(10) Danset, D.; Manceron, L. *J. Phys. Chem. A* **2003**, *107*, 11324−11330.

(11) Kometer, R.; Legay, F.; Legay-Sommaire, N.; Schwentner, N. *J. Chem. Phys.* **1994**, *100*, 8737−8745.

(12) Frisch, M. J.; Trucks, G. W.; Schlegel, H. B.; et al. *Gaussian 03*, revision B.02; Gaussian, Inc.: Pittsburgh, PA, 2003.

(13) Adamo, C.; Barone, V. *J. Chem. Phys.* **1998**, *108*, 664−675.

(14) Lynch, B. J.; Fast, P. L.; Harris, M.; Truhlar, D. G. *J. Phys. Chem. A* **2000**, *104*, 4811−4815.

(15) Zhao, Y.; Lynch, B. J.; Truhlar, D. G. *J. Phys. Chem. A* **2004**, *108*, 2715−1719.

(16) Zhao, Y.; Truhlar, D. G. *J. Phys. Chem. A* **2004**, *108*, 6908−6918.

(17) Krishnan, R.; Binkley, J. S.; Seeger, R.; A Pople, J. *J. Chem. Phys.* **1980**, *72*, 650−654.

(18) Clark, T.; Chandrasekhar, J.; Spitznagel, G. W.; Schleyer, P. v. R. *J. Comput. Chem.* **1983**, *4*, 294−301.

(19) Frisch, M. J.; Pople, J. A.; Binkley, J. S. *J. Chem. Phys.* **1984**, *80*, 3265−3269.

(20) Huber, K. P.; Herzberg, G. *Molecular Spectra and Molecular Structure Constant of Diatomic Molecules*; Van Nostrand Reinhold: New York, 1979.

(21) NIST Computational Chemistry Comparison and Benchmark Database, NIST Standard Reference Database Number 101, Release 12, August 2005; Johnson III, R. D., Ed. http://srdata.nist.gov/cccbdb.

(22) Krokidis, X.; Silvi, B.; Alikhani, M. E. *Chem. Phys. Lett.* **1998**, *292*, 35−45.

(23) Locht, R.; Leyh, B.; Hoxha, A.; Dehareng, D.; Jochims, H. W.; Baumgärtel, H. *Chem. Phys.* **2001**, *272*, 277−292.